Nonlinear transfer function encodes synchronization in a neural network from the mammalian brain

L. Menendez de la Prida[1,*] and J. V. Sanchez-Andres[2]

[1]*Unidad de Cartografia, Instituto Pluridisciplinar, Universidad Complutense, Paseo Juan XXIII, 1, 28040 Madrid, Spain*
[2]*Instituto de Bioingenieria, Universidad Miguel Hernandez, Campus de San Juan Apartado 18, 03550 Alicante, Spain*

Synchronization is one of the mechanisms by which the brain encodes information. The observed synchronization of neuronal activity has, however, several levels of fluctuations, which presumably regulate local features of specific areas. This means that biological neural networks should have an intrinsic mechanism able to synchronize the neuronal activity but also to preserve the firing capability of individual cells. Here, we investigate the input-output relationship of a biological neural network from developing mammalian brain, i.e., the hippocampus. We show that the probability of occurrence of synchronous output activity (which consists in stereotyped population bursts recorded throughout the hippocampus) is encoded by a sigmoidal transfer function of the input frequency. Under this scope, low-frequency inputs will not produce any coherent output while high-frequency inputs will determine a synchronous pattern of output activity (population bursts). We analyze the effect of the network size (N) on the parameters of the transfer function (threshold and slope). We found that sigmoidal functions realistically simulate the synchronous output activity of hippocampal neural networks. This outcome is particularly important in the application of results from neural network models to neurobiology. [S1063-651X(99)03809-X]

PACS number(s): 87.19.La, 87.10.+e, 07.05.Kf

Neuronal integration is one of the most important mechanisms of the brain. By its means a considerable amount of information is continuously processed in a large number of internal operations. An intriguing question in neuronal integration is how large populations of neurons encode information; in particular, how synchronized patterns of neural activity emerge. Synchronization is the basis of stimulus detection, of spontaneous activity driving developmental processes, and of pathological states such as epilepsy [1]. The brain contains several nuclei that are involved in specific functions, such as the thalamus, the olfactory bulb, or several cortical areas. Despite their intrinsic properties, these nuclei constitute neural networks with input and output pathways that interact with each other during processing. It has been suggested that the selective synchronization of these areas serves as a mechanism of binding distributed information into a complete representation [2]. It is, therefore, important to understand how the properties of external stimuli determine the pattern and degree of synchronization within a network, i.e., its input-output relationship.

Historically, the sigmoidal transfer function has been computed from the input-output relationship of individual neurons and subsequently applied to neural network models [3]. A network extension of the sigmoidal dependence is not strictly correct since such a generalization assumes homogeneity and linear interactions among cells. In particular, the input-output relationship from individual neurons is obtained by applying intracellular current pulses of different amplitudes, a procedure that is not experimentally possible at network level. Instead, extracellular stimulation is applied but its strength has not a quantitative physiological interpretation. Recent experimental reports have shown that neurons

individually encode information according to the stimulus frequency from sigmoidal dependency to band-pass filtering [4,5]. The extent to which these particular transfer functions can be extrapolated to the network should be thus experimentally investigated. Here we examined the input-output relationship of realistic neural networks using hippocampal slices from newborn rabbits as an experimental model of synchronous firing [6]. The hippocampal circuit has been compared with an autoassociative neural network, showing computational properties such as content addressable memory [7]. This made hippocampal slices particularly suitable to investigate the properties of biological networks [Fig. 1(a)]. In this study, we compute the input-output relationship of hippocampal networks by stimulating the input pathway at constant stimulus amplitude but at several frequencies [8], while simultaneously recording the activity from principal cells (cornu Ammon regions 1 and 2, CA3 and CA1 neurons). The effect of network size is investigated by preparing minislices of several lengths. We then use the transfer function to estimate the network output by simulating the CA1 firing probability (real output) using CA3 spontaneous activity as the input signal. We compare the results from simulation with the network activity recorded in the output area (CA1).

A schematic representation of the experimental system is represented in Fig. 1(b). Hippocampal slices (500-μm thick) were prepared following the standard procedure [9]. Simultaneous recordings at CA3 and CA1 were made from the cell body layer while stimulating the input pathway at the mossy fibers [9]. The synchronous network response between CA3 and CA1 depended on the input frequency f [Fig. 2(a)]. This synchronous network response consisted in a population burst, which was tightly synchronous in proximal cells and propagated from CA3 (recording site 1) to CA1 (recording site 2). Single or repetitive stimulation at 1–6 Hz did not induce a synchronous response whatever the stimulus duration. Instead, synchronization was systematically elicited

---

*Author to whom correspondence should be addressed. Electronic address: liset@eucmax.sim.ucm.es
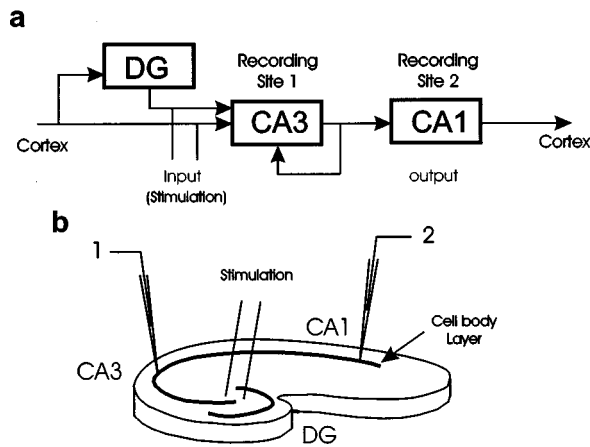
FIG. 1. (a) Schematic diagram of the hippocampus. Input pathways from the cortex made synaptic contacts at the dentate gyrus (DG) and CA3. Stimulation of the input fibers was made at this level where synaptic connections (mossy fibers) from DG to CA3 were also stimulated. CA3 send its axons (forward) to CA1 and CA3 properly (backward). Axons from CA1 provide the hippocampal output to the cortex. Recordings were made from CA3 (recording site 1) and CA1 (recording site 2). (b) Schematic representation of the hippocampal slices with the stimulation and recording electrodes (1 and 2).

from 9–10 Hz (threshold). It is important to note that this is not a problem of frequency coupling between the network response and the stimulus. In hippocampal slices, the synchronous network response consists of a stereotyped population burst where duration, number of spikes, and interspike interval, remains nearly constant [4]. These stereotyped bursts emerged synchronously between recording sites 1 and 2, which means that the entire hippocampal network fires as a whole (synchronous output) depending on the particular conditions of the input, i.e., its frequency. To quantify this neuronal synchronization the coherence for the simultaneous recordings 1 and 2 was computed. Coherence K_{12} for two signals is equal to the average cross-power spectrum normalized by the averaged power spectrum of the compared signals,

$$K_{12} = \frac{|C_{xy}|^2}{C_{xx}C_{yy}}. \qquad (1)$$

Coherence is the frequency domain equivalent to the cross-covariance function and is a measure of the similarity of two signals. Its value lies between zero and one and it estimates the degree to which phases at the frequency of interest are dispersed.

We represented coherence between recording sites 1 and 2 against input frequency to quantify the degree of network synchronization as a function of the stimulus [Fig. 2(b)]. For stimulus frequencies $f<6$ Hz the coherence was near zero indicating low correlations between the recording sites 1 and 2. On the contrary, frequencies higher than 9 Hz evoked synchronization across the entire hippocampal slice, which was reflected in maximal values of coherence (>0.5). At intermediate frequency values between 6–9 Hz, large fluctuations were detected compared with small and large values of f. If we define the coefficient of variation as the ratio
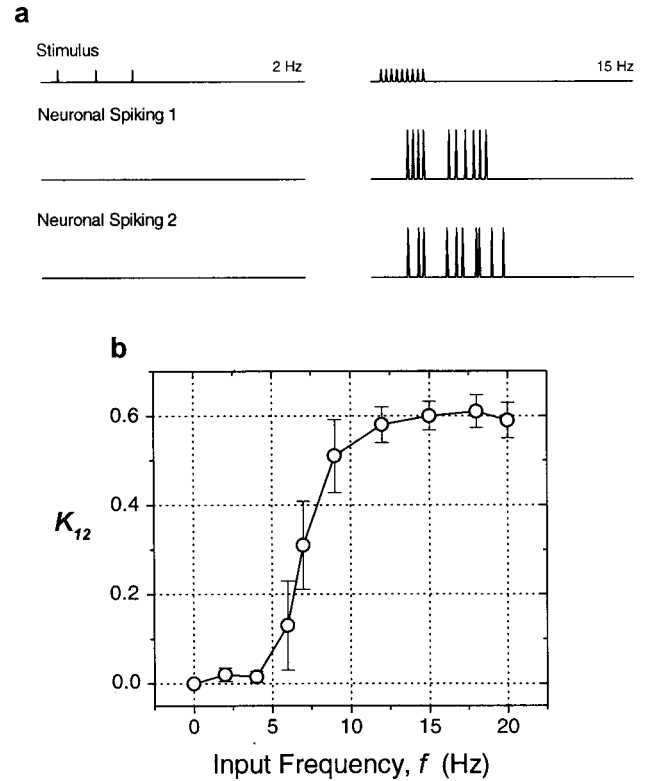

FIG. 2. (a) Synchronous response of the hippocampal network to periodical stimulus. Repetitive stimulation induces synchronous population events (bursts) at recording sites 1 and 2 only at frequencies higher than 9 Hz. (b) Coherence versus the input frequency. Highest coherence values were obtained at $f>10$ Hz. In the midrange ($6<f<9$ Hz) large fluctuations were observed.

between the coherence standard deviation and the mean (σ/μ) it is found that for $6<f<9$ Hz, $(\sigma/\mu)=0.411 \pm 0.123$ while for $f<6$ Hz and $f>10$ Hz $(\sigma/\mu)=0.062 \pm 0.007$. This effect is reported in theoretical simulations of hippocampal networks [10] and reflects the fluctuating number of active neurons that are recruited by the external stimulus in the midrange.

To obtain the network transfer function we computed the probability of synchronous firing between recording sites 1 and 2 for several input frequencies. Based on the previous analysis we defined synchronization between recording sites 1 and 2 when coherence values were larger than 0.5 [Fig. 2(b)]. By using this criteria we computed the probability of synchronous output activity between recording sites 1 and 2, $P(f)$, for every stimulus frequency f. Data were obtained from $n=11$ different hippocampal slices and could be well fitted by a sigmoidal function [Fig. 3],

$$P(f) = \frac{1}{1 + e^{f - f_0/\Delta}}, \qquad (2)$$

where f_0 and Δ represent the threshold and the slope, respectively; $f_0 = 8.8 \pm 0.1$ Hz and $\Delta = 0.9 \pm 0.1$ Hz. We analyzed the effect of the network size (N) on the input-output relationship by constructing minislices from a 300–2500-μm length. In slices, CA3 and CA1 areas are estimated to have 10 000 and 16 500 neurons, respectively [11]. Assuming that CA3 is a 1000-μm length, this means that a 300-μm minis-
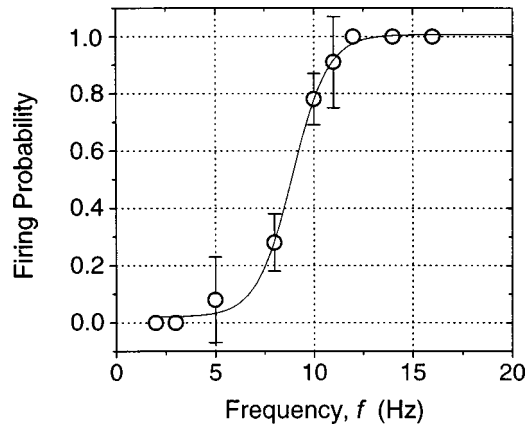
FIG. 3. Transfer function from $n = 11$ hippocampal slices. Data can be well fitted by a sigmoidal function [Eq. (2)] where $f_0 = 8.8 \pm 0.1$ Hz and $\Delta = 0.9 \pm 0.1$ Hz.

lice should contain the order of 3000 neurons. We prepared minislices of a 300, 600, and 1000-μm length from CA3 area and of a 2000–2500-μm length from CA1 area and recorded simultaneously from two different sites. The results are presented in Fig. 4 (data from $n = 18$ minislices). As can be seen f_0 (circles) increased, as network size became smaller. This means that for small networks the input-output function shifted towards higher-frequency values. In terms of the activity this result suggests that smaller networks are more difficult to synchronize, a result that is in accordance with experimental and theoretical reports [12]. In fact, realistic computational models of hippocampal slices have shown that in networks of $N = 25-100$ neurons synchronous bursts are no longer recorded [13].

On the contrary, the slope of the transfer function (Δ) is reduced by a factor of 15 as N is decreased [Fig. 4, triangles]. This means that for small networks ($N < 5000$) the transfer function becomes more abrupt, i.e., small frequency changes will produce larger variations of output firing probability than for networks of $N > 15\,000$. In computer simulations, N is usually smaller than biological network sizes and steplike transfer functions are frequently used. Results in Fig. 4 show that steplike functions have a physiological support for small networks, though the extension of results based in computation with such a function should be carefully justified.
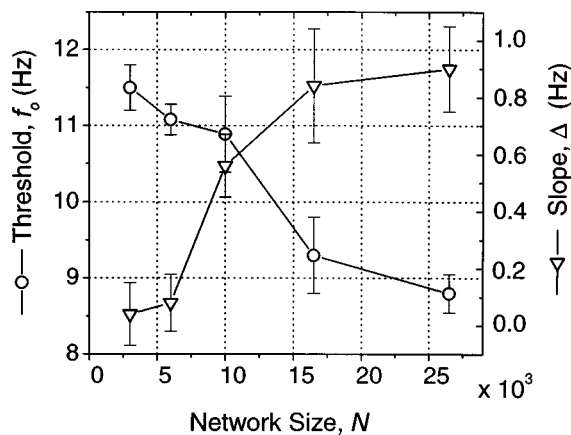

FIG. 4. Dependence of threshold (f_0) and slope (Δ) of the transfer function with the network size (N).
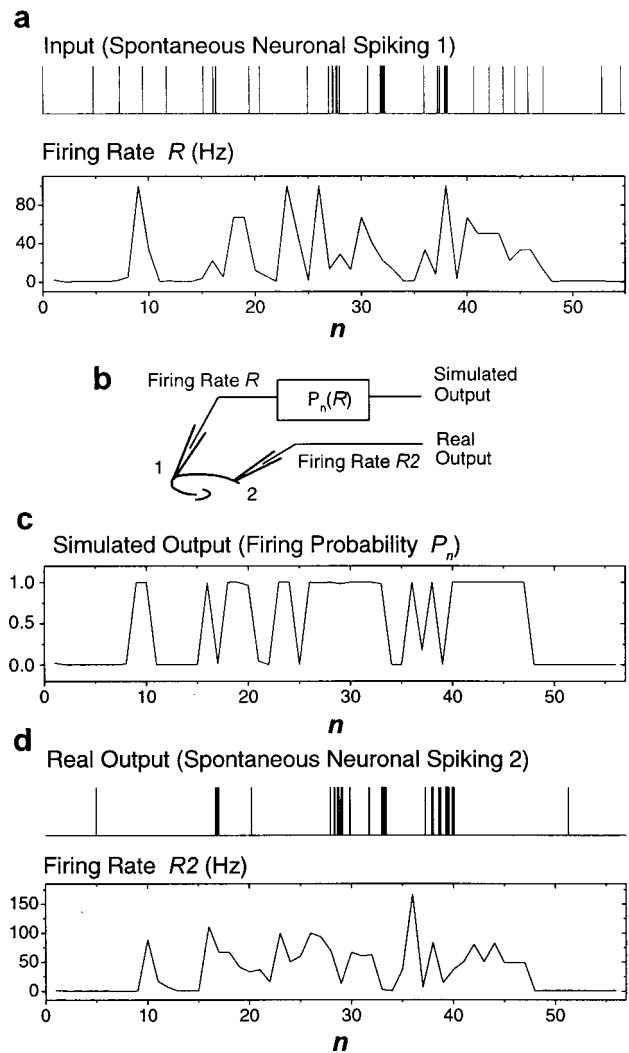

FIG. 5. Simulation of the network output by the sigmoidal transfer function and comparison with the real output activity recorded at CA1. 1(a) CA3 spontaneous neuronal activity 1, i.e., the activity recorded in the absence of stimulus was used as the input signal in the sigmoidal transfer function. To do this we constructed time series from neuronal spiking 1 by computing the firing rate in Hz (R_n), i.e., the inverse of the interspike interval. (b) Schematic representation of the analysis. Five to ten minutes of spontaneous neuronal spiking at CA3 (recording site 1) was converted into a time series of $n = 50-60$ length (firing rate R) and applied to Eq. (2) thus obtaining the simulated output, i.e., the firing probability P_n. The simulated output is then compared to the real output recorded at site 2 (transformed into firing rate $R2$). (c) Simulated output obtained from Eq. (2) using firing rate 1 as the input frequency $f = R$. (d) Real output recorded at CA1 (site 2). The neuronal spiking 2, which was recorded simultaneously to neuronal spiking 1, can be converted into a time series of firing rate 2 or firing probability as well.

Finally, we tested the capacity of the network transfer function [Eq. (2)] to predict the real pattern of output activity. To perform this test we used the spontaneous firing of CA3 neurons as the input signal. The CA3 spontaneous firing is the activity recorded at site 1 (neuronal spiking 1) in the absence of any stimulus. We converted the neuronal spiking 1 into a time series by computing the firing rate in Hz (R), i.e., the inverse of the interspike intervals [Fig. 5(a);
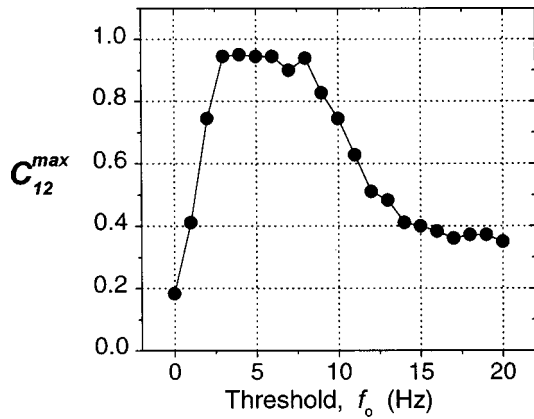
FIG. 6. Correlation between the simulated and the real output activity depending on the synchronization threshold f_0. The maximum of the cross-correlation function was computed for each value of f_0. Results are presented in normalized form.

put signals) were suprathreshold thus determining an output response. For f_0 between 9–20 Hz the sigmoidal function is shifted towards high-frequency values and, therefore, the output pattern is almost silent, i.e., the majority of spontaneous spiking fluctuations are subthresholds. Cross correlation was maximum for $3 < f_0 < 8$ Hz indicating a strong correlation between the simulated and the real network behavior.

In summary, all these results indicate that transfer function (2) realistically simulate the input-output properties of hippocampal neural networks and can be used for computational purposes in an adaptive tuning threshold from 3–8 Hz. Interestingly, these frequencies are in the range of theta rhythm, i.e., 4–8 Hz [14], which has been found to be optimal for the induction of long-term potentiation [15]. A number of theoretical studies have been carried out to investigate the storage capacity of the neural networks with a sigmoidal input-output relationship [16]. This connection between experimental models of memory and their theoretical counterparts deserves more attention, especially on the view that information storage is coded in patterns of activity at 5–12 Hz and 40 Hz [17].

Another important result from this work is that in biological neural networks synchronization (in the form of population bursts) is encoded by a nonlinear function of the input frequency. On this basis a network filtering capability can be proposed, which would determine the existence of two modes of signaling [18]. Input frequencies below threshold (<8 Hz) will not produce any coherent output, having network activity largely variable. This intrinsic variability is found to be important in coding the local features of specific areas [19]. In fact, it has been apparent that the irregularity of a neuronal firing pattern enhances the detection of weak stimulus via stochastic resonance [20]. On the contrary, input frequencies higher than threshold will determine a synchronized pattern of output activity within the network (>8 Hz). Large-scale oscillations in this range have been reported in the visual cortex [21], olfactory system[22], thalamus [23], and hippocampus [24]. In these systems, 40-Hz oscillations have been suggested to serve as a mechanism of binding the neuronal activity from distributed networks [2,25]. This means that biological networks should have an internal mechanism able to both produce synchronized patterns of neuronal activity and preserve the individual firing capacity of the neurons. The sigmoidal network function of input frequency provides a solution to this problem by playing the role of a functional switch between these two operational modes.

see also the scheme in Fig. 5(b)]. These time series $(R_1, R_2, \ldots, R_n)$ had a length that is equivalent to the number of spikes (n) in the original signal. We have analyzed epochs of 5–10 minutes of recording time which gave firing rate time series of 50–60 length. Then, Eq. (2) was applied to simulate the output activity of the hippocampal network by using firing rate 1 as the input frequency, $f_n = R_n$, thus obtaining the simulated output time series, i.e., the firing probability P_n [Fig. 5(c)]. The simulated output P_n was compared with the real output activity (neuronal spiking 2 and firing rate 2) recorded at site 2, i.e., from CA1 neurons [Fig. 5(d)].

The sigmoidal transfer function characterized by the parameters f_0 and Δ reported in Fig. 3 successfully simulate the output activity of hippocampal slices. To quantify the degree of correlation between the simulated and the real output activity, the cross-correlation function from these two signals was computed:

$$C_{12}(\tau) \Leftrightarrow [x(t) - \langle x \rangle][y(t + \tau) - \langle y \rangle], \qquad (3)$$

where $\Leftrightarrow$ is the inverse Fourier transform, [] denotes the Fourier transform, $\langle \rangle$ denotes the mean, []' represents the complex conjugate, and x and y are the simulated and real output (firing probability), respectively. We investigated the dependence between the maximum of the cross-correlation function ($C_{12}^{\max}$) and the threshold of the transfer function (f_0) [Fig. 6]. For thresholds ranging from 0–2 Hz and from 9–20 Hz simulated and real network outputs were not correlated. In the first interval ($0 < f_0 < 2$ Hz), the sigmoidal function is shifted towards low-frequency values so low that the simulated output activity was maximal, i.e., all of the spontaneous spiking fluctuations from CA3 cells (used as the in-

[1] C. M. Gray and W. Singer, Proc. Natl. Acad. Sci. USA **91**, 1872 (1989); G. Laurent and H. Davidowitz, Science **265**, 1872 (1994); M. Meister, R. O. L. Wong, D. A. Baylor, and C. Shatz, *ibid.* **252**, 939 (1991) P. A. Schwartzkroin and D. A. Prince, Brain Res. **147**, 117 (1978).

[2] A. K. Engel, P. Köning, A. K. Kreiter, T. B. Schillen, and W. Singer, Trends Neurosci. **15**, 218 (1992).

[3] J. P. Segundo, D. H. Perkel, H. Wyman, H. Hegstad, and G. P. Moore, Kybernetik **4**, 157 (1968); D. R. Chialvo, A. Longtin, and J. Müller-Gerking, Phys. Rev. E **55**, 1798 (1997).

[4] L. Menendez de la Prida and J. V. Sanchez-Andres, J. Neurophysiol **82**, 209 (1999).

[5] T. Gloveli, D. Schmitz, R. M. Empson, and U. Heinemann, J. Neurophysiol. **78**, 3444 (1997).

[6] L. Menendez de la Prida, S. Bolea, and J. V. Sanchez-Andres, Neurosci. Lett. **218**, 185 (1996).

[7] T. Konohen, *Self-Organization and Associative Memory* (Spinger-Verlag, Berlin, 1984).

[8] The stimulation protocol was established at the beginning of every experiment. The stimulus amplitude was kept constant at the minimal value able to produce a synaptic response (known as postsynaptic potential). Ten to twenty trials of repetitive stimulation from 0 to 20 Hz were tested.

[9] Transverse slices of hippocampus from newborn rats and rabbits (2–5 postnatal days), 500 μm in thickness, were prepared using a drop-blade chopper. For recording, one slice was transferred to a submerged-type recording chamber (Medical Systems) continuously perfused with the standard perfusion medium (in mM: 125 NaCl, 3 KCl, 1.2 $MgSO_4$, 1.2 NaH_2PO_4, 2 $CaCl_2$, 22 $NaHCO_3$, and 10 glucose, saturated with 95% O_2-5% CO_2, pH: 7.4). Recording electrodes were made from borosilicate glass (outer diameter, 1.2 mm, Sutter Instrument Co.) pulled with a Brown-Flaming horizontal puller (Sutter Instrument Co.), and filled with 3M KCl (50–100 MΩ). Simultaneous intracellular recordings were made with separated manipulators using a dual intracellular amplifier (Axoclamp II B). Monopolar electrical stimulation was applied via tungsten electrodes at mossy fibers simultaneously with intracellular recordings. The stimulus duration was 100 μs. See [8] for more details on the stimulation protocol.

[10] R. D. Traub and R. Dingledine, J. Neurophysiol. **64**, 1009 (1990).

[11] C. Bernard and H. V. Wheal, Hippocampus **4**, 497 (1994).

[12] R. Miles, R. K. S. Wong, and R. D. Traub, Neuroscience **12**, 1179 (1984); K. L. Smith, D. H. Szarowski, J. N. Turner, and J. W. Swann, J. Neurophysiol. **74**, 650 (1995); R. D. Traub and R. Miles, *Neuronal Networks of the Hippocampus* (Cambridge University Press, Cambridge, 1991).

[13] R. D. Traub, W. D. Knowles, R. Miles, and R. K. S. Wong, Neuroscience (NY) **12**, 1191 (1984).

[14] I. Soltesz and M. Deschenes, J. Neurophysiol. **70**, 97 (1993).

[15] Long-term potentiation (LTP) is a mechanism by which repetitive stimulation of a fiber enhances its excitatory synaptic contacts. It has been proposed to be a form of memory; see R. A. Nicoll, J. A. Kauer, and R. C. Malenka, Neuron **1**, 97 (1988); J. Larson, D. Wong, and R. Lynch, Brain Res. **368**, 347 (1986).

[16] J. J. Hopfield, Proc. Natl. Acad. Sci. USA **81**, 3088 (1984); D. J. Amit, H. Gutfreund, and H. Sompolinsky, Phys. Rev. A **32**, 1007 (1985); S. Grossberg, Neural Networks **1**, 17 (1988).

[17] L. Ingber, Phys. Rev. E **52**, 4561 (1995); J. E. Lisman and M. A. P. Idiart, Science **267**, 1512 (1995).

[18] L. Menendez de la Prida, N. Stollenwerk, and J. V. Sanchez-Andres, Physica D **110**, 323 (1997).

[19] R. R. de Ruyter van Steveninck, G. D. Lewen, S. P. Strong, R. Koberle, and W. Bialek, Science **275**, 1805 (1997); S. P. Strong, R. Koberle, R. R. de Ruyter van Steveninck, and W. Bialek, Phys. Rev. Lett. **80**, 197 (1998); G. Deco and B. Schürmann, *ibid.* **79**, 4697 (1997); M. N. Shaden and W. T. Newsome, J. Neurosci. **18**, 3870 (1998); A. Arieli, A. Sterkin, A. Grinvald, and A. Aertsen, Science **273**, 1868 (1996); W. Bair and C. Koch, Neural Comput. **8**, 1185 (1996).

[20] J. J. Collins, C. C. Chow, and T. T. Imhoff, Phys. Rev. E **52**, R3321 (1995); J. J. Collins, T. T. Imhoff, and P. Grigg, J. Neurophysiol. **76**, 642 (1996); F. Moss, J. K. Douglass, L. Wilkens, D. Pierson, and E. Pantazelou, Ann. N.Y. Acad. Sci. **706**, 26 (1993); B. J. Gluckmann, T. I. Netoff, E. J. Neel, W. L. Ditto, M. L. Spano, and S. J. Schiff, Phys. Rev. Lett. **77**, 4098 (1996).

[21] C. M. Gray, P. Köning, A. K. Engel, and W. Singer, Nature (London) **388**, 334 (1989); R. Eckhorn, Biol. Cybern. **60**, 121 (1988); D. Hansel and H. Sompolinski, J. Comput. Neurosci. **3**, 7 (1996).

[22] W. J. Freeman, *Mass Action in the Nervous System* (Academic, New York, 1975); G. Laurent, Trends Neurosci. **19**, 489 (1996).

[23] D. Contreras, A. Destexhe, T. J. Sejnowski, and M. Steriade, Science **278**, 771 (1996); U. Kim, M. Sanchez-Vives, and D. A. McCormick, *ibid.* **278**, 130 (1997).

[24] R. D. Traub and R. Miles, Science **243**, 1319 (1989); M. A. Whittington, R. D. Traub, and J. G. R. Jefferys, Nature (London) **373**, 612 (1995); X. J. Wang and G. Buzsáki, J. Neurosci. **16**, 6402 (1996).

[25] R. Llinas and U. Ribary, Proc. Natl. Acad. Sci. USA **90**, 2078 (1993).